A Switched System Dwell-Time Update Mechanism for Path Following With Intermittent State Feedback Constraints

Duc M. Le, Andrew R. Teel, *Fellow, IEEE*, and Warren E. Dixon, *Fellow, IEEE*

***Abstract*— This article focuses on a class of problems where a switched system approach is used to model intermittencies in state feedback. Specifically, a single-agent with nonlinear dynamics is tasked with following a desired path that lies in a feedback-denied region where state feedback is unavailable. As a result, the agent must use open-loop state estimates (dead-reckon) to navigate along the desired path while periodically returning to a known feedback region where the accumulated dead-reckoning errors are regulated. A dwell-time update mechanism is developed that leverages intermittent data measurements to generate a relaxed dwell-time condition in comparison to previous literature. The updated dwell-time conditions are used to plan the duration spent following the desired path before returning to the feedback region to acquire state feedback. A Lyapunov-based switched system dwell-time analysis is used to show the state tracking error is uniformly ultimately bounded to a prescribed error threshold that also guarantees re-entry of the agent to the feedback region. Comparative numerical simulations are conducted to demonstrate the efficacy of the developed method.**

***Index Terms*—Dead reckoning, Lyapunov methods, nonlinear control, switched systems.**

I. Introduction

Autonomous systems are often tasked with objectives such as state regulation, trajectory tracking, and multi-agent coordination. To accomplish such objectives, control designs critically depend on a system's ability to continuously acquire and use state feedback. However, factors such as the task definition, operating environment, sensor modality, and adversarial attacks may impede continuous state sensing capabilities. Moreover, relaxing continuous state acquisition requirements can improve autonomous system design by reducing costs such as energy consumption, computational demands, and required hardware devices such as GPS.

Motivated to obviate the need for continuous state feedback, various methods have been developed that tolerate intermittencies in state feedback. For example, in visual servoing applications, approaches have been developed to address the practical problem when landmarks or image features leave the field of view. In results such as [1], a daisy-chaining approach is used to link features that leave the image with features that remain visible for position and pose estimation. Similarly, simultaneous localization and mapping algorithms have been developed to generate local state estimates in feature-rich environments (cf., [2], [3], [4]). In the context of communication networks, unreliable communication channels may result in delays and intermittent losses of information. The results in [5], [6], and [7] model temporary losses in communication as a random process and use Kalman filtering with intermittent observations. Moreover, to conserve resources such as communication energy and bandwidth, self- and event-triggered mechanisms have been developed where sensing and actuation are executed discretely based on a trigger condition (cf., [8] and [9]).

Emerging results in [10], [11], [12], [13], [14], [15], and [16] examined a class of problems where a switched system approach was used to model the intermittencies in state feedback (see Fig. 1).

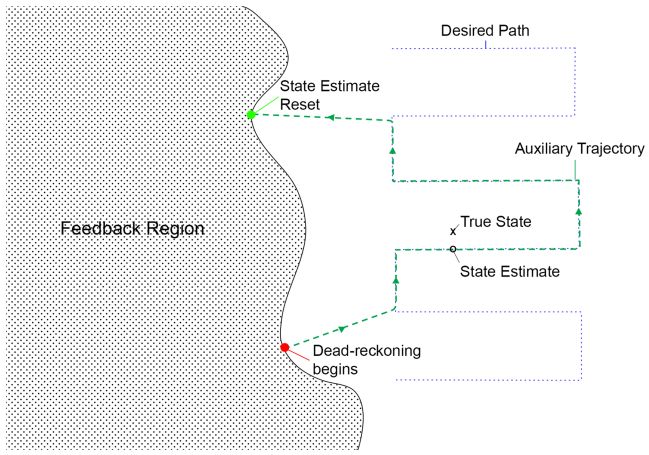

Fig. 1. Illustration of the single-agent switched system intermittent feedback approach. The feedback region is shown in the black dotted area. State measurements are available to the agent while inside the feedback region, otherwise it is unavailable. The desired path is indicated by the blue dashed line. Since state measurements are not continuously available, the agent must follow a user-defined auxiliary trajectory shown in the green dashed line. The auxiliary trajectory is designed such that it directs the agent from the feedback region to the desired path, then it directs the agent along the desired path until it departs the desired path to return to the feedback region. Upon leaving the feedback region (red dot), the agent dead-reckons (uses open-loop state estimates) to navigate along the auxiliary trajectory. At an instant in time outside the feedback region, the open-loop state estimate and true state of an autonomous agent are illustrated by the black circle and x markers, respectively. The discrepancy between the state estimate and the true state represents the dead-reckoning error. To regulate the dead-reckoning error, the auxiliary trajectory directs the agent back to the feedback region (green dot) where the agent may acquire state measurements and reset the state estimate. Note that the problem formulation can be extended to multiagent problems using the Relay-Explorer framework (see [11]).

Manuscript received 15 November 2023; accepted 20 January 2024. Date of publication 6 February 2024; date of current version 28 June 2024. This work was supported in part by ONR project under Grant N000142112481 and in part by AFOSR under Grant FA9550-19-1-0169, Grant FA9550-22-1-0429, and Grant FA9550-21-1-0452. Recommended by Associate Editor S. Galeani. *(Corresponding author: Duc M. Le.)*

Duc M. Le is with the Aurora Flight Sciences, a Boeing Company, Cambridge, MA 02142 USA (e-mail: le.duc@aurora.aero).

Andrew R. Teel is with the Department of Electrical and Computer Engineering, University of California, Santa Barbara, CA 93106 USA (e-mail: teel@ece.ucsb.edu).

Warren E. Dixon is with the Department of Mechanical and Aerospace Engineering, University of Florida, Gainesville, FL 32611 USA (e-mail: wdixon@ufl.edu).

Digital Object Identifier 10.1109/TAC.2024.3362865

Specifically, the results such as [10], [15], and [16] examined switched systems with two modes of operation: 1) a stabilizable mode where state feedback is available and 2) a potentially unstable mode where state feedback is unavailable. When state measurements are available, feedback controllers are used to stabilize the system, otherwise open-loop state estimates (dead-reckoning) are used to navigate when state measurements are unavailable. Lyapunov-based switched system methods in [17], [18], and [19] are used to analyze the closed-loop state tracking error of the switched system, and to develop sufficient dwell-time conditions on the switching signal. The developed dwell times are sufficient conditions that determine the maximum duration the system can endure without state feedback, and the minimum duration required in the stabilizing mode. Specifically, the maximum dwell time is derived from a guaranteed re-entry criterion that ensures the tracking errors do not exceed a specified threshold that is sufficient to guarantee the agent reacquires state feedback. The minimum dwell time ensures the tracking errors are regulated to a desired threshold before exiting the feedback available mode. Similarly, time-based constraints on the switching signal have also been studied for general switched nonlinear systems and hybrid systems in results such as [20], [21], [22], [23], [24], [25], [26], [27], and [28]. The results in [23] considered switched nonlinear systems with unstable modes and used an average dwell-time condition and introduced a time-ratio constraint to guarantee input/output-to-state-stability. The average dwell-time condition limits the frequencies of switches while the time-ratio constraint limits the duration the unstable modes are active. Results in [24] used a hybrid systems approach to induce the time-ratio constraint from [23] using an auxiliary timer state to develop a time-ratio monitor that limited the duration the unstable modes wer active. In addition, the time-ratio monitor was used in conjunction with an average dwell-time automaton in results such as [26], [27], and [28] for hybrid systems with unstable modes. Although the time-based constraints on the switching signal in the aforementioned results and in this article both provide stability certificates, the maximum dwell-time condition (i.e., the maximum duration in the unstable mode) developed in this article is derived from a guaranteed re-entry criterion and is independent of the stable mode.

The switched system intermittent feedback framework introduced in [10] considered a single-agent system tasked with following a path that lay in a feedback-denied environment. Therefore, the agent must dead-reckon along the desired path while repeatedly returning to a known feedback region to acquire state feedback and regulate the accumulated dead-reckoning errors. Similarly, results in [12] extended the intermittent path following framework in [10] to a class of nonholonomic systems tasked with exploration of uncertain environments. In addition, the results in [11] and [13] extended the switched system intermittent feedback framework to a multiagent coordination setting where a leader agent with local state sensing capabilities must relay state feedback to the remaining agents by moving within proximity of the follower agents' communication radius.

The results in [10], [11], [12], [13], [14], [15], and [16] used Lyapunov-based techniques to develop dwell-time conditions based on conservative bounds. Consequently, the aforementioned results yield conservative dwell-time conditions that require a system to acquire state feedback more frequently than required. Moreover, the results in [10], [11], [12], [13], [14], [15], and [16] limited the dwell-time analysis to circular feedback regions, which also restricted the dwell time. As a result, recent efforts have been made to relax the dwell-time condition. The results in [29] built on the switched system framework in [10] by examining criteria under which an agent is guaranteed to re-enter a feedback region with arbitrary geometry. A topologically inspired method is used to factor in geometric parameters of a known feedback region and provide sufficient conditions for guaranteed re-entry. The sufficient conditions are used to develop a path-planning algorithm that computes a relaxed dwell-time condition. However, the improvement in the dwell time is dependent on the geometry of the feedback region. Overall, the dwell-time analyses in [29] and the results such as [10], [11], [12], [13], [14], [15], and [16] were limited by conservative bounds on the system dynamics. Hence, the preliminary results in [15] incorporated an extremum seeking control method that used intermittent measurements to update the dwell-time condition.

This article builds on the switched system framework in [10] and the preliminary results in [15], which consider a single-agent nonlinear system subject to exogenous disturbances that is tasked with following a desired path that lies in a region where state measurements are unavailable (see Fig. 1). A new dwell-time update mechanism is developed to relax the dwell-time condition. Unlike previous results, the developed dwell-time update mechanism leverages intermittent data measurements of the dead-reckoning error to iteratively adjust the dwell-time condition. In comparison, for the result in [10], the dwell-time condition is static and dependent on conservative bounds. A Lyapunov-based analysis is used to analyze the switched system dynamics resulting from intermittencies in state measurements. The developed dwell-time conditions guarantee the agent re-enters the feedback region and also ensures the state tracking error is uniformly ultimately bounded to a prescribed error threshold. In addition, the developed dwell-time update algorithm is analyzed to guarantee the generated dwell-time conditions are less conservative than the nominal dwell time developed in prior works in [10] and [15].

II. Problem Formulation

A. Switched System Framework

This section introduces the switched system framework in [10] for path following subject to intermittencies in state measurements. This article considers a single-agent system that is capable of measuring its state $x : \mathbb{R}_{\geq 0} \to \mathbb{R}^n$ while inside a known feedback region. The feedback region is a known set of states where state measurements are available to the agent; otherwise, state measurements are unavailable (see Fig. 1). In this article, the feedback region is defined as the set $\mathscr{F} \triangleq \{x \in \mathbb{R}^n : \|x - x_c\| \leq R\} \subseteq \mathbb{R}^n$, where $R > 0$ denotes a known constant, and $x_c \in \mathbb{R}^n$ denotes a known fixed vector. The agent is tasked with following a desired path that lies entirely outside of the feedback region. In addition, due to the lack of state measurements while outside the feedback region, the agent must dead-reckon (i.e., use state estimates $\hat{x} : \mathbb{R}_{\geq 0} \to \mathbb{R}^n$) to navigate along the desired path.[1] Hence, a state-dependent switching controller and state estimator are designed such that state measurements are used when available, and state estimates are used when state measurements are unavailable.

To facilitate the subsequent development, let a and u be indices denoting modes of a switched system (subsystems) when state measurements are available and unavailable, respectively. Let $\mathscr{P} \triangleq \{a, u\}$ denote the set of operating modes of the switched system. Let $p : \mathbb{R}_{\geq 0} \to \mathscr{P}$ denote a piecewise right-continuous switching signal that indicates the active subsystem. Let the concatenated state $z : \mathbb{R}_{\geq 0} \to \mathbb{R}^{2n}$ be defined as $z \triangleq [x^T, \hat{x}^T]^T$. A switched controller $v_p : \mathbb{R}^{2n} \times \mathbb{R}_{\geq 0} \to \mathbb{R}^n$

[1] Visual odometry or the use of inertial measurements may reduce the growth rate of the state estimate over traditional open-loop estimates without any feedback measurements. However, without absolute sensing (e.g., "loop-closure" with visual odometry), the measurements may drift and lead to instability. Hence, such methods can also be included in the generalized concept of "open-loop dead-reckoning" considered in this article.

and state estimator are designed as

$$v_p(z,t) \triangleq \begin{cases} v_a(x,t), & p=a, \\ v_u\left(\hat{x},t\right), & p=u, \end{cases} \tag{1}$$

$$\dot{\hat{x}} \triangleq \begin{cases} f(x,t)+v_a(x,t)+\tilde{v}(z,t), & p=a, \\ f\left(\hat{x},t\right)+v_u\left(\hat{x},t\right), & p=u, \end{cases} \tag{2}$$

where the functions $(x,t)\mapsto v_a(x,t)$ and $(\hat{x},t)\mapsto v_u(\hat{x},t)$ denote the control laws when state feedback is available and unavailable, respectively; $(z,t)\mapsto \tilde{v}(z,t)$ denotes a state feedback term, and $f:\mathbb{R}^n\times\mathbb{R}_{\geq 0}\to\mathbb{R}^n$ denotes the agent's locally Lipschitz drift dynamics. The switched system framework allows for various controller and state estimator designs in (1) and (2), provided sufficient Lyapunov-like conditions (introduced subsequently in Section III) are satisfied. Then, the single-agent system is modeled as a switched nonlinear system

$$\dot{x} = f(x,t)+v_p(z,t)+d(t) \tag{3}$$

where $d:\mathbb{R}_{\geq 0}\to\mathbb{R}^n$ denotes an unknown exogenous disturbance. For simplicity, the development in this article considers fully actuated systems (see [12] for extensions to systems with nonholonomic constraints). The following assumption facilitates the subsequent development.

Assumption 1: The exogenous disturbance $t\mapsto d(t)$ is a class $\mathscr{C}^1$ function, and there exists known constants $\delta,\gamma\in\mathbb{R}_{>0}$ such that $d(\cdot)$ and its time derivative $\dot{d}(\cdot)$ can be bounded as $\|d(t)\|\leq\delta$ and $\|\dot{d}(t)\|\leq\gamma$ for all $t\in\mathbb{R}_{\geq 0}$, respectively.

B. Control Objective

The potential instabilities from dead-reckoning motivate the switched system intermittent path following approach introduced in [10] that is adopted in this article, i.e., "loop-closure" by returning to a region of the state-space where absolute measurements are available. The path following task is expressed as a time-based trajectory tracking problem for an auxiliary trajectory that is designed to ensure the path is followed, while also ensuring the agent returns to the feedback region in sufficient time. Specifically, the control objective is to track a user-defined auxiliary trajectory $x_\sigma:\mathbb{R}_{\geq 0}\to\mathbb{R}^n$ that coincides with the desired path and repeatedly returns to the feedback region to regulate the dead-reckoning errors. To quantify the tracking objective, an error system is defined as

$$e \triangleq x-x_\sigma, \quad \hat{e}\triangleq\hat{x}-x_\sigma, \quad \tilde{e}\triangleq x-\hat{x} \tag{4}$$

where $e:\mathbb{R}_{\geq 0}\to\mathbb{R}^n$ denotes the state tracking error, $\hat{e}:\mathbb{R}_{\geq 0}\to\mathbb{R}^n$ denotes the state estimate tracking error, and $\tilde{e}:\mathbb{R}_{\geq 0}\to\mathbb{R}^n$ denotes the state estimate error. Using (1)–(3) and taking the time derivatives of the error system in (4) yields a family of closed-loop error dynamics of the forms

$$\dot{e}=g_{e,p}(z,t), \quad \dot{\hat{e}}=g_{\hat{e},p}(z,t), \quad \dot{\tilde{e}}=g_{\tilde{e},p}(z,t) \tag{5}$$

for all $p\in\mathscr{P}$, where $g_{e,p},g_{\hat{e},p},g_{\tilde{e},p}:\mathbb{R}^{2n}\times\mathbb{R}_{\geq 0}\to\mathbb{R}^n$.

III. Dwell-Time Analysis

In this section, the framework in [10] is used to develop a relaxed maximum loss of feedback availability condition that dictates the maximum duration the agent can remain outside the feedback region. Similarly, to guarantee the reacquisition of state measurements, the normalized state tracking error is required to be bounded by a user-defined maximum error threshold upon entering the feedback region.[2] The maximum dwell-time condition in [10] is introduced and used as a nominal dwell-time condition for initialization. A new dwell-time update mechanism is then developed that uses intermittent output measurements of the agent upon returning to the feedback region to update the dwell-time condition. The resulting switched system generated by the class of switching signals admitted by the updated dwell-time conditions is analyzed to ensure reentry of the agent into the feedback region. Moreover, the developed algorithm is analyzed to show the generated dwell times are less conservative than the nominal dwell time developed previously in [10].

To facilitate the subsequent analysis, the following notation is introduced. Let $t_i^a\geq 0$ for all $i\in\mathbb{Z}_{\geq 0}$ denote the ith instant when p switches from u to a, i.e., the instant the agent enters the feedback region. For the complementary case, let $t_i^u\geq 0$ for all $i\in\mathbb{Z}_{\geq 0}$ denote the ith instant when the switching signal p switches from a to u, i.e., the instant the agent exits the feedback region. Based on the switching instants, the dwell times $\Delta t_i^a\triangleq t_i^u-t_i^a$ and $\Delta t_i^u\triangleq t_{i+1}^a-t_i^u$ for all $i\in\mathbb{Z}_{\geq 0}$ denote the ith activation of the subsystems a and u.

To analyze the closed-loop error system in (5), candidate Lyapunov-like functions are defined as

$$V_e(e)\triangleq\frac{1}{2}e^Te, \qquad V_{\hat{e}}\left(\hat{e}\right)\triangleq\frac{1}{2}\hat{e}^T\hat{e}, \qquad V_{\tilde{e}}\left(\tilde{e}\right)\triangleq\frac{1}{2}\tilde{e}^T\tilde{e} \tag{6}$$

where $V_e,V_{\hat{e}},V_{\tilde{e}}:\mathbb{R}^n\to\mathbb{R}_{\geq 0}$. To facilitate the subsequent dwell-time analysis, the following assumption is made.

Assumption 2: [10] Consider the family of systems in (5). Based on the design of the control input and state estimator in (1) and (2), respectively, the following inequalities hold:

$$\left\langle\frac{\partial V_e}{\partial e},g_{e,a}(z,t)\right\rangle\leq-2\lambda_eV_e, \tag{7}$$

$$\left\langle\frac{\partial V_{\hat{e}}}{\partial \hat{e}},g_{\hat{e},u}(z,t)\right\rangle\leq-2\lambda_{\hat{e}}V_{\hat{e}}, \tag{8}$$

$$\left\langle\frac{\partial V_{\tilde{e}}}{\partial \tilde{e}},g_{\tilde{e},p}(z,t)\right\rangle\leq\begin{cases}-2\lambda_{\tilde{e},a}V_{\tilde{e}}, & p=a,\\ 2\lambda_{\tilde{e},u}V_{\tilde{e}}+\frac{\delta^2}{2}, & p=u,\end{cases} \tag{9}$$

where $\lambda_e,\lambda_{\hat{e}},\lambda_{\tilde{e},a},\lambda_{\tilde{e},u}\in\mathbb{R}_{\geq 0}$ are known constants, and δ is a known constant that was introduced in Assumption 1.[3]

Based on the definitions of the switching indices introduced above (6), the feedback available subsystem $p(t)=a$ coincides to the time interval $t\in[t_i^a,t_i^u)$ for all $i\in\mathbb{Z}_{\geq 0}$, and the feedback unavailable mode $p(t)=u$ corresponds to the time interval $t\in[t_i^u,t_{i+1}^a)$ for all $i\in\mathbb{Z}_{\geq 0}$. This shorthand notation is used in (7)–(9) and the remainder of this article. The inequalities in Assumption 2 ensure bounds on the closed-loop error signals in (5) that are used to develop a maximum loss of feedback dwell-time condition. Therefore, this framework allows for various controller and state estimator designs that satisfy Assumption 2 (see [10, Sec. VI] for a design example). Using the definition of $V_{\hat{e}}$ and $V_{\tilde{e}}$ in (6) and applying the Comparison Lemma [30, Lemma 3.4] to (8) and (9) yields

$$\|\hat{e}(t)\|\leq\|\hat{e}\left(t_i^u\right)\|\exp\left(-\lambda_{\hat{e}}\left(t-t_i^u\right)\right),\forall t\in[t_i^u,t_{i+1}^a), \tag{10}$$

[2]The developed method in this article also considers circular feedback regions for simplicity and to better focus the result on the unique specific contributions. The topologically inspired method in [29] can be used with the developed method to extend to feedback regions with generic geometries.

[3]Under the switched system framework adopted in this article, the control and state estimator designs are decoupled from the stability analysis. See Section IV for a concrete design example of (1) and (2) that satisfy the criteria specified in Assumption 2.

$$\|\tilde{e}(t)\|^2 \leq \tilde{c}\left(t_i^u\right)\exp\left(2\lambda_{\tilde{e},u}\left(t-t_i^u\right)\right)-\frac{\delta^2}{2\lambda_{\tilde{e},u}}, \forall t\in[t_i^u, t_{i+1}^a) \tag{11}$$

respectively, where $\tilde{c}(t_i^u) \triangleq \|\tilde{e}(t_i^u)\|^2 + \frac{\delta^2}{2\lambda_{\tilde{e},u}}$ for all $i \in \mathbb{Z}_{\geq 0}$ is an auxiliary variable. While the agent is inside the feedback region, state measurements can be used to update the auxiliary trajectory and state estimate as $x_\sigma(t) = x(t)$ and $\hat{x}(t) = x(t)$ for all $t \in [t_i^a, t_i^u)$, respectively. Hence, at the instant the agent re-enters the feedback region, the following resets are applied:

$$x_\sigma(t_i^a) = x(t_i^a),\ \hat{x}(t_i^a) = x(t_i^a) \tag{12}$$

for all $i \in \mathbb{Z}_{\geq 0}$, i.e., the auxiliary trajectory and state estimate are updated based on the re-entry location to regulate the dead-reckoning errors rather than remaining inside the feedback region for a specified amount of time before returning to the desired path. Hence, the agent can instantaneously leave the feedback region (i.e., $t_i^a = t_i^u$) upon applying the resets in (12). To distinguish states at the reset times, consider a piecewise continuous function $t \mapsto h(t)$ with discontinuities occurring at reset times t_i^a and t_i^u. At the reset times t_i^u, $h(t_i^u) \triangleq \lim_{t\to t_i^{u+}} h(t)$ denotes the function after the resets are applied. Similarly, $h(t_i^a) \triangleq \lim_{t\to t_i^{a-}} h(t)$ denotes the function before the resets are applied. Therefore, applying the reset maps yields $\|e(t_i^u)\| = \|\hat{e}(t_i^u)\| = \|\tilde{e}(t_i^u)\| = 0$ for all $i \in \mathbb{Z}_{\geq 0}$. Using (4), the error e can be expressed as $e = \hat{e} + \tilde{e}$. Then, using (10) and (11) and applying the resets yields

$$\|e(t)\| \leq \left[\frac{\delta^2}{2\lambda_{\tilde{e},u}}\left(\exp\left(2\lambda_{\tilde{e},u}\left(t-t_i^u\right)\right)-1\right)\right]^{\frac{1}{2}} \quad \forall t\in[t_i^u, t_{i+1}^a). \tag{13}$$

The inequality in (13) is a bound on the normalized state tracking error while the agent is outside the feedback region (i.e., $t \in [t_i^u, t_{i+1}^a)$), and is used to develop the nominal dwell-time condition $\Delta t_{\text{nom}}^u \in \mathbb{R}_{>0}$ in the following theorem.

Theorem 1: [10, Th. 1] Consider an agent modeled by the dynamics in (3) with initial condition $x(\tau_0) \in \mathscr{F}$ and $\tau_0 \geq 0$, and suppose Assumptions 1 and 2 hold. The composite error system trajectories of the switched system generated by the family of subsystems described in (5) with a piecewise, right-continuous switching signal $t \mapsto p(t) \in \mathscr{P}$ are uniformly ultimately bounded in the sense that $\|e(t)\| \leq e_M$ for all $t > \tau_0 + \tau$ with $\tau > 0$, provided the switching signal satisfies the sufficient maximum loss of feedback dwell-time condition

$$\Delta t_i^u = \Delta t_{\text{nom}}^u \leq \frac{1}{2\lambda_{\tilde{e},u}}\ln\left(\frac{2\lambda_{\tilde{e},u}e_M^2}{\delta^2}+1\right) \tag{14}$$

$\forall i \in \mathbb{Z}_{\geq 0}$, where $e_M \in \mathbb{R}_{>0}$ is a user-defined parameter,[4] and the known constants $\lambda_{\tilde{e},u}$ and δ were previously defined in (9).

Remark 1: The nominal dwell-time condition in (14) is sufficient to guarantee the agent's state tracking error does not exceed the maximum error threshold e_M, which also guarantees re-entry to the feedback region. Similar to (13), a convergence bound on the normalized state tracking error while the agent is inside the feedback region can be developed and used to develop a minimum feedback availability dwell-time condition [10, Th. 1]:

$$\Delta t_i^a \geq \frac{-1}{\min\{\lambda_e, \lambda_{\tilde{e},a}\}}\ln\left(\min\left\{\frac{e_m}{\|e(t_i^a)\|+\|\tilde{e}(t_i^a)\|}, 1\right\}\right)$$

for all $i \in \mathbb{Z}_{\geq 0}$, where $e_m \in \mathbb{R}_{>0}$ denotes a user-defined parameter and the known constants λ_e and $\lambda_{\tilde{e},a}$ were previously defined in Assumption 2. However, by applying the reset maps described in (12), the dead-reckoning errors can be regulated instantly, eliminating the minimum dwell-time condition.

[4]The guaranteed re-entry criterion in [10] required selecting the maximum error threshold e_M to be less than or equal to the radius of the feedback region.

Algorithm 1: Dwell-Time Update Mechanism.

Output: Maximum dwell-time condition update Δt_{i+1}^u

Input:

Initialize $\Delta t_0^u = \Delta t_{nom}^u = \frac{1}{2\lambda_{\tilde{e},u}}\ln(\frac{2\lambda_{\tilde{e},u}e_M^2}{\delta^2}+1)$

Require δ, γ, $\lambda_{\tilde{e},u}$, and e_M

1: **if** Agent enters feedback region, i.e., $t = t_{i+1}^a$ **then**

2: Compute output measurement $y_i = \|e(t_{i+1}^a)\|$

3: Compute $\delta_i = [\frac{2\lambda_{\tilde{e},u}y_i^2}{\exp(2\lambda_{\tilde{e},u}\Delta t_i^u)-1}]^{\frac{1}{2}}$ and $\hat{\delta}_i = \delta_i + \gamma\Delta t_i^u$

4: Compute

$\chi_1 = [\frac{1}{2\lambda_{\tilde{e},u}}\ln(\frac{2\lambda_{\tilde{e},u}}{\delta^2}(e_M - \|e(t_i')\|)^2+1)]$,

$\chi_2 = \frac{\delta-\hat{\delta}_i}{\gamma} - \Delta t_i^u$, and $\Delta t_i' \leq \min(\chi_1, \chi_2)$

5: Dwell-time update $\Delta t_{i+1}^u = \Delta t_i^u + \Delta t_i'$

6: **return** Δt_{i+1}^u

The nominal dwell time in (14) is used to initialize the algorithm which updates the dwell time based on the intermittent measurements in (15). The updated dwell time is analyzed in Theorem 2 and guarantees the state tracking error is bounded. Subsequently, the developed algorithm is analyzed in Lemma 1 to show that the updated dwell time is less conservative than the nominal dwell time under Assumption 3.

In Theorem 1, the nominal dwell-time condition developed in (14) is used for initialization during the initial instance the agent leaves the feedback region, i.e., $\Delta t_0^u = \Delta_{\text{nom}}^u$. In [10], the dwell-time condition ensured the dead-reckoning error did not exceed the error threshold e_M. Upon re-entry to the feedback region, the agent acquires state measurements that provide information on how conservative the dwell time is, i.e., the discrepancy between the true and allowable dead-reckoning error. Despite having intermittent data on the dead-reckoning errors, the dwell-time analysis in Theorem 1 yields a constant dwell time and is dependent on conservative bounds on the modeled dynamics. Consequently, the conservative dwell time requires the agent to allocate more time returning to the feedback region, which inhibits the agent's ability to follow the desired trajectory. Hence, this motivates the development of a new algorithm that incorporates the intermittent measurements acquired upon re-entry to the feedback region.

To quantify the intermittent measurements, a discrete output measurement $y_i : \mathbb{Z}_{\geq 0} \to \mathbb{R}_{>0}$ is defined as

$$y_i \triangleq \left\|e\left(t_{i+1}^a\right)\right\| \quad \forall i \in \mathbb{Z}_{\geq 0}. \tag{15}$$

The output measurement provides a measure of the true dead-reckoning error during the ith instance the agent returns to the feedback region. Using intermittent output measurements in (15), relaxed dwell-time conditions are generated in the subsequently developed dwell-time update mechanism in Algorithm 1. The dwell-time update mechanism in Algorithm 1 also generates sufficient dwell-time conditions on the switching signal. The resulting class of switched systems admitted are analyzed to show boundedness of the state tracking error in the following theorem.

Theorem 2: Consider an agent modeled by the dynamics in (3) with initial condition $x(\tau_0) \in \mathscr{F}$ and $\tau_0 \geq 0$, and suppose Assumptions 1 and 2 hold. The dwell-time update mechanism described in Algorithm 1 ensures the error system trajectories of the switched system generated

by the family of subsystems described in (5) are uniformly ultimately bounded.

Proof: Based on (13) and (15), let $\delta_i : \mathbb{Z}_{\geq 0} \to \mathbb{R}_{>0}$ be defined as

$$\delta_i \triangleq \left[\frac{2\lambda_{\tilde{e},u} y_i^2}{\exp\left(2\lambda_{\tilde{e},u}\Delta t_i^u\right) - 1}\right]^{\frac{1}{2}} \tag{16}$$

for all $i \in \mathbb{Z}_{\geq 0}$. Using (16), a discrete auxiliary variable $\hat{\delta}_i : \mathbb{Z}_{\geq 0} \to \mathbb{R}_{\geq 0}$ is defined as

$$\hat{\delta}_i \triangleq \delta_i + \gamma \Delta t_i^u \tag{17}$$

where γ is defined in Assumption 1. Let $t_i' \triangleq t_i^u + \Delta t_i^u$, where $t_i' : \mathbb{Z}_{\geq 0} \to (t_i^u, t_{i+1}^a)$ denotes an intermediate time instant while the agent is outside the feedback region. Using (13) and (17) yields

$$\|e\left(t_i'\right)\| \leq \left[\frac{\hat{\delta}_i}{2\lambda_{\tilde{e},u}}\left(\exp\left(2\lambda_{\tilde{e},u}\Delta t_i^u\right) - 1\right)\right]^{\frac{1}{2}}. \tag{18}$$

Using (13) and (18), the agent's state tracking error bound yields

$$\|e\left(t_{i+1}^a\right)\| \leq \left[\frac{\delta^2}{2\lambda_{\tilde{e},u}}\left(\exp\left(2\lambda_{\tilde{e},u}\Delta t_i'\right) - 1\right)\right]^{\frac{1}{2}} + \|e\left(t_i'\right)\| \tag{19}$$

where $\Delta t_i' \triangleq t_{i+1}^a - t_i'$. To guarantee re-entry of the agent to the feedback region, it is required that the normalized state tracking error is bounded by the maximum allowable error while outside the feedback region, i.e., $[\frac{\delta^2}{2\lambda_{\tilde{e},u}}(\exp(2\lambda_{\tilde{e},u}\Delta t_i') - 1)]^{\frac{1}{2}} + \|e(t_i')\| \leq e_M$. Then, solving the inequality in (19) for $\Delta t_i'$ yields

$$\Delta t_i' \leq \frac{1}{2\lambda_{\tilde{e},u}} \ln\left(\frac{2\lambda_{\tilde{e},u}}{\delta^2}\left(e_M - \|e\left(t_i'\right)\|\right)^2 + 1\right). \tag{20}$$

The inequality constraint in (20) represents the additional duration of time the agent can extend during the next iteration of leaving the feedback region. The inequality in (20) is derived from the bound on the normalized state tracking error in (19) which incorporates information on the exogenous disturbance using the discrete measurements in (16). Based on the discrete measurements in (16) and known bounds on the disturbance from Assumption 1, the following inequality constraint must also be satisfied:

$$\Delta t_i' \leq \frac{\delta - \delta_i}{\gamma} - \Delta t_i^u. \tag{21}$$

Therefore, satisfying both (20) and (21) yields the following inequality constraint:

$$\Delta t_i' \leq \min\left(\chi_1, \chi_2\right) \tag{22}$$

where $\chi_1 \triangleq [\frac{1}{2\lambda_{\tilde{e},u}} \ln(\frac{2\lambda_{\tilde{e},u}}{\delta^2}(e_M - \|e(t_i')\|)^2 + 1)]$ and $\chi_2 \triangleq \frac{\delta - \delta_i}{\gamma} - \Delta t_i^u$ for all $i \in \mathbb{Z}_{\geq 0}$ are measurable terms. Then, using (22), the dwell-time update mechanism is designed as

$$\Delta t_{i+1}^u = \Delta t_i^u + \Delta t_i' \tag{23}$$

for all $i \in \mathbb{Z}_{\geq 0}$. If the switching signal satisfies the maximum dwell-time condition in (23), then by construction of the dwell-time update mechanism, the normalized state tracking error is bounded as $\|e(t)\| \leq e_M$ for all $t \in [t_i^u, t_{i+1}^a)$ and $i \in \mathbb{Z}_{\geq 0}$. ■

In Theorem 2, Algorithm 1 is analyzed and guaranteed to generate dwell times that ensure the normalized state tracking error is bounded by the maximum allowable threshold error. In the following lemma, Algorithm 1 is analyzed to ensure the generated dwell times are less conservative than the nominal dwell-time condition in (14). To facilitate the subsequent analysis, the following assumption is made.[5]

Assumption 3: Given known parameters δ and γ from Assumption 1 and a nominal dwell time Δt_{nom}^u defined in (14), the controller in (1) can be designed to yield $\lambda_{\tilde{e},u}$, defined in (9), such that the following inequality is satisfied

$$\frac{\delta}{\gamma} - \frac{1}{\gamma}\left[\frac{2\lambda_{\tilde{e},u} e_M^2}{\exp\left(2\lambda_{\tilde{e},u}\Delta t_i^u\right) - 1}\right]^{\frac{1}{2}} \geq \Delta t_{nom}^u \quad \forall i \in \mathbb{Z}_{\geq 0}. \tag{24}$$

Lemma 1: Suppose Assumptions 1–3 hold. The dwell-time update mechanism described in Algorithm 1 ensures that

$$\Delta t_{i+1}^u \geq \Delta t_{nom}^u \quad \forall i \in \mathbb{Z}_{\geq 0}. \tag{25}$$

Proof: Substituting (22) into (23), the dwell-time update mechanism yields

$$\Delta t_{i+1}^u = \Delta t_i^u + \min\left(\chi_1, \chi_2\right) \tag{26}$$

where χ_1 and χ_2 were defined below (22). Based on (26), there are two possible cases for the dwell-time update mechanism. In the first case, if $\frac{1}{2\lambda_{\tilde{e},u}} \ln(\frac{2\lambda_{\tilde{e},u}}{\delta^2}(e_M - \|e(t_i')\|)^2 + 1) \leq \frac{\delta - \delta_i}{\gamma} - \Delta t_i^u$, then the dwell-time update in (26) yields

$$\Delta t_{i+1}^u = \Delta t_i^u + \frac{1}{2\lambda_{\tilde{e},u}} \ln\left[\frac{2\lambda_{\tilde{e},u}}{\delta^2}\left(e_M - \|e\left(t_i'\right)\|\right)^2 + 1\right]. \tag{27}$$

In (27), the bracketed term is nonnegative. Hence, (27) can be lower bounded as $\Delta t_{i+1}^u \geq \Delta t_i^u$ for all $i \in \mathbb{Z}_{\geq 0}$. By Algorithm 1, the dwell-time condition is initialized as $\Delta t_0^u = \Delta t_{\text{nom}}^u$. Then, according to the recursive relation in (27) with initial condition $\Delta t_0^u = \Delta t_{\text{nom}}^u$, the dwell-time update mechanism satisfies (25). In the second case, if $\frac{1}{2\lambda_{\tilde{e},u}} \ln(\frac{2\lambda_{\tilde{e},u}}{\delta^2}(e_M - \|e(t_i')\|)^2 + 1) > \frac{\delta - \delta_i}{\gamma} - \Delta t_i^u$, the dwell-time update in (26) yields

$$\Delta t_{i+1}^u = \frac{\delta}{\gamma} - \frac{1}{\gamma}\delta_i. \tag{28}$$

Substituting (16) into (28) yields

$$\Delta t_{i+1}^u = \frac{\delta}{\gamma} - \frac{1}{\gamma}\left[\frac{2\lambda_{\tilde{e},u} y_i^2}{\exp\left(2\lambda_{\tilde{e},u}\Delta t_i^u\right) - 1}\right]^{\frac{1}{2}}. \tag{29}$$

By Theorem 1, the nominal dwell-time condition Δt_{nom}^u in (14) ensures the state tracking error is bounded as $\|e(t)\| \leq e_M$ for all $t \in \mathbb{R}_{\geq 0}$. Similarly, by Theorem 2, the dwell-time update mechanism ensures the state tracking error is bounded as $\|e(t)\| \leq e_M$ for all $t \in \mathbb{R}_{\geq 0}$. Therefore, by (15), y_i can be bounded as $0 \leq y_i \leq e_M$, for all $i \in \mathbb{Z}_{\geq 0}$. Hence, (29) can be lower bounded as

$$\Delta t_{i+1}^u \geq \frac{\delta}{\gamma} - \frac{1}{\gamma}\left[\frac{2\lambda_{\tilde{e},u} e_M^2}{\exp\left(2\lambda_{\tilde{e},u}\Delta t_i^u\right) - 1}\right]^{\frac{1}{2}} \quad \forall i \in \mathbb{Z}_{\geq 0}. \tag{30}$$

Then, (25) follows from Assumption 3 and (30). ■

IV. Numerical Simulations

To demonstrate the performance of the developed dwell-time update mechanism in Algorithm 1, simulations were conducted. In the simulation results, the feedback region was modeled as $\mathcal{F} = \{x \in \mathbb{R} : \|x\| \leq$

[5]The inequality in (24) of Assumption 3 is restrictive and may not be possible to satisfy for some systems, e.g., systems with small magnitude disturbances with high rates of change. However, there is a large class of systems that can satisfy the verifiable sufficient condition in (24) (see the numerical simulations in Section IV for an example).

$0.5\}$. The controller in (1) was designed as

$$v_p \triangleq \begin{cases} \dot{x}_\sigma - k_e e - f(x,t) - k_s \text{sgn}(e), & p = a, \\ \dot{x}_\sigma - k_{\hat{e}} \hat{e} - f(\hat{x},t), & p = u \end{cases} \tag{31}$$

where $k_e, k_{\hat{e}}, k_s \in \mathbb{R}_{\geq 0}$ are user-defined parameters. The state estimator in (2) was designed as follows [10]:

$$\dot{\hat{x}} \triangleq \begin{cases} f(x,t) + v_a(t) + k_{\tilde{e}} \tilde{e} + k_s \text{sgn}\left(\tilde{e}\right), & p = a, \\ f(\hat{x},t) + v_u(t), & p = u \end{cases} \tag{32}$$

where $k_{\tilde{e}} \in \mathbb{R}_{\geq 0}$ is a user-defined parameter.[6] Similar to [10, Sec. VI], x_σ was designed with the smootherstep function.

A. Simulation Configurations

To demonstrate and gain insight on the performance of the dwell-time update mechanism in Algorithm 1, three simulation cases were conducted for 240 s. For simplicity, in all simulation cases, a scalar system (i.e., $n = 1$) in (3) was considered with drift dynamics $f(x) \triangleq x$, for all $x \in \mathbb{R}$. The desired path is selected as $x_d(t) = 2$ for all $t \in \mathbb{R}_{\geq 0}$. The control parameters for the controller in (31) and state estimator in (32) were selected as $k_e = k_{\hat{e}} = 1$, $k_{\tilde{e}} = 1.1$, and $k_s = 0.26$. The state and state estimate were initialized as $x(0) = 0.4$ and $\hat{x}(0) = 0$, respectively. The user-defined parameter $e_M = 0.5$ was used throughout all simulation cases.

In Case 1, a baseline simulation was conducted using the nominal dwell-time condition in (14) with the known bounds $\delta = 0.2$ and $\lambda_{\tilde{e},u} = 1.5$. Note that the nominal dwell-time condition does not use the bound $\dot{\delta}$. The disturbance in (3) was modeled as $d(t) = 0.05$, $\forall t \in \mathbb{R}_{\geq 0}$. In the second case, a similar simulation was conducted using the same disturbance model in Case 1. However, the developed algorithm was used and examined in two separate subcases. Specifically, in Case 2a, Algorithm 1 was implemented with the known bounds $\delta = 0.2$, $\gamma = 0.01$, and $\lambda_{\tilde{e},u} = 1.5$. Case 2b follows similarly, but with the known bound $\gamma = 0.001$. Subcases "a" and "b" were conducted to examine how variations in the known bounds of the disturbance and its time derivative affect the performance of the developed algorithm. Finally, two additional subcases were examined in Case 3a and Case 3b using Algorithm 1 with the same parameters and bounds as in Case 2a and Case 2b, respectively. However, instead of a constant disturbance, a time-varying disturbance was modeled as $d(t) = 0.035 + 0.015 \sin(0.03t - 45) h_\tau(t)$, where $h_\tau : \mathbb{R}_{\geq 0} \to \{0, 1\}$ denotes the Heaviside function defined as $h_\tau(t) = \begin{cases} 1, & t \geq 45, \\ 0, & \text{else}, \end{cases}$ $\forall t \in \mathbb{R}_{\geq 0}$.

The known bounds of the disturbances in all cases was 0.2. The known bounds of the time derivative of the disturbances corresponding to Cases 2a, 2b, 3a, and 3b were 0.01, 0.001, 0.01, and 0.001, respectively. Note that model knowledge of the disturbances was not used in the control and state estimator design. Only the known bound on the disturbance, by Assumption 1, was used for control gain tuning. Moreover, the parameters used in the simulation study satisfied the stated assumptions. Practically, knowledge of the bounds of the disturbance in the stated assumptions is typically application dependent and varies based on how much uncertainty there is in the disturbance and its time derivative.

B. Results and Discussion

Recall the auxiliary trajectory x_σ was designed according to the dwell-time condition Δt_i^u, i.e., the duration of the trajectory outside the feedback region was dependent on Δt_i^u. To illustrate the implications of the extended dwell times generated by the developed dwell-time update mechanism, Fig. 2 illustrates the state trajectories resulting from the nominal dwell-time condition in (14) (Case 1), and the dwell-time update mechanism in Algorithm 1 (Case 2b). As expected, from approximately 3 to 4.9 s, the state trajectories coincide as the dwell-time in Algorithm 1 was initialized as the nominal dwell time ($\Delta t_{\text{nom}}^u = 0.99$ s). However, after the initial re-entry to the feedback region, the dwell time in Case 2b was updated to $\Delta t_1^u = 1.81$ s—a nearly twofold increase compared to the nominal dwell time. As a result, the agent returned to the feedback region less often as seen from approximately 4.9–6.8 s where the trajectory for the baseline Case 1 returned to the feedback region twice, whereas the trajectory returned once in Case 2b.

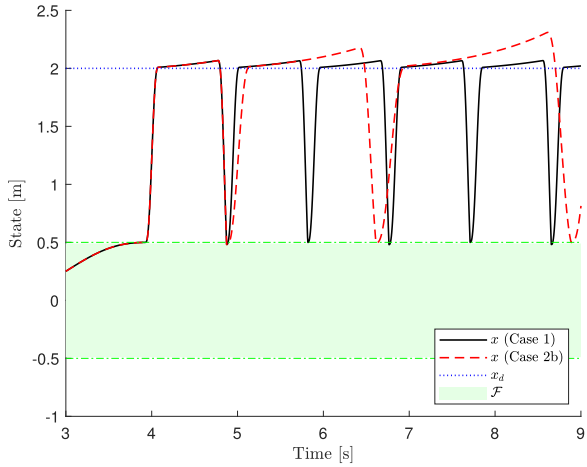

Fig. 2. Evolution of the state trajectories from 3 to 9 s. The feedback region is shown in the shaded green region. The state x (Case 1) using the nominal dwell time in (14) is shown in the solid black line. The state x (Case 2b) using Algorithm 1 is shown in the dashed red line.

Remark 2: In Fig. 2, the resulting dwell times from Algorithm 1 yield reduced performance in the tracking of the desired path. The level of precision in the tracking performance can be prescribed by the selection of the maximum error threshold e_M. However, there is a tradeoff between the prescribed level of precision and the maximum dwell time. To emphasize the main contribution of this article, e_M was selected as the worst-case threshold error that sufficiently guaranteed re-entry of the agent to the feedback region.

Fig. 3 illustrates the evolution of the disturbances against the evolution of the dwell time for each of the simulation cases. During the initial instance outside the feedback region from approximately 4–5 s, the dwell time was $\Delta t_0^u = 0.99$ s for all simulation cases. The dwell time in the baseline simulation of Case 1 remained constant over the duration of the simulation due to the nominal dwell-time condition being static. However, the dwell times in Cases 2a, 2b, 3a, and 3b increased, on average, by approximately twofold to 1.92, 2.27, 2.04, and 2.55 s, respectively. Relative to the nominal dwell time in Case 1, the dwell times in Cases 2a, 2b, 3a, and 3b increased by 193%, 228%, 206%, and 256%, respectively. From approximately 5–45 s, the dwell times had a transient period of increase until a steady state was reached across all cases. In Case 2, the dwell times remain at a steady state for the entire duration of the simulation, as expected with a constant disturbance. However, the disturbance in Case 3 increased after 45 s as the sinusoidal component was activated. Despite the variation in the disturbance in Case 3, the dwell-time update mechanism in both Cases 3a and 3b was able to adapt accordingly, i.e., as the magnitude of the disturbance increased, the dwell time decreased, and vice versa.

[6]By taking the time derivatives of (6), using (5), and substituting (31) and (32), it can be shown Assumption 2 is satisfied.

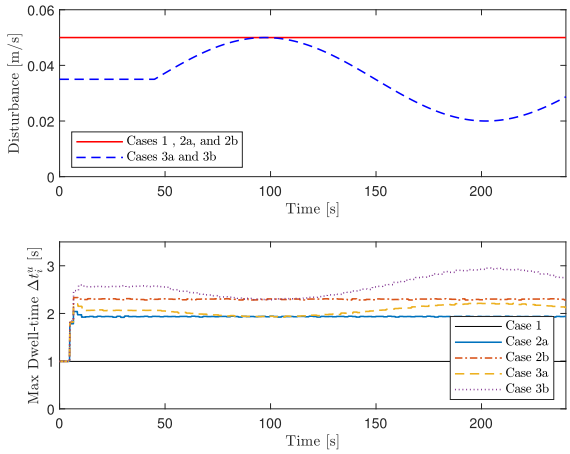

Fig. 3. (Top): Evolution of the disturbances $d(t)$. The constant disturbance for Cases 1 and 2 is shown in the solid red line. The time-varying disturbance for Case 3 is shown in the dashed blue line. (Bottom): Evolution of the dwell time Δt_i^u for each of the simulation cases. Note that the dwell time was updated discretely and is constant until re-entry to the feedback region.

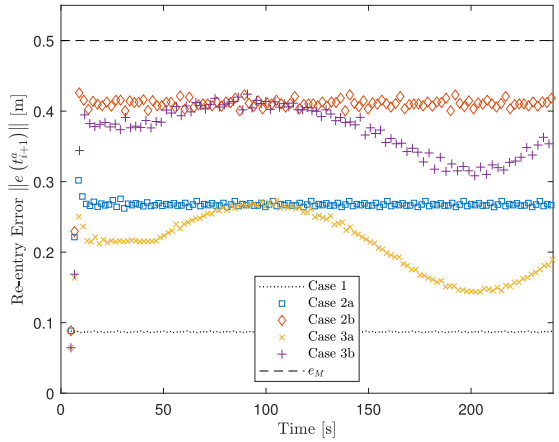

Fig. 4. Evolution of the normalized state tracking error $\|e(t_{i+1}^a)\|$ at each time instant of re-entry to the feedback region for each of the simulation cases. The maximum error threshold e_M is shown in the dashed black line.

Relative to the corresponding "a" subcases, the dwell times in Cases 2b and 3b were larger by 118% and 125%, respectively.

Fig. 4 illustrates the agent's normalized tracking (dead-reckoning) error at each instant of re-entry to the feedback region. As stated in Remark 2, the selected maximum error threshold $e_M = 0.5$ in the dashed black line represents the guaranteed re-entry criterion. Re-entry error values below e_M indicate the possibility of the agent remaining outside the feedback region for a longer duration. In Case 1, the re-entry error is the lowest among the cases and resided at a constant $\|e(t_{i+1}^u)\| = 0.09$, which is 17% of the maximum allowed error. Using the dwell-time update mechanism in Cases 2 and 3, the re-entry errors increased while not exceeding the maximum error threshold. Ideally, the maximum dwell time would yield a re-entry error of $\|e(t_{i+1}^u)\| = e_M$. However, the developed algorithm accounts for variations in the disturbance, hence the re-entry errors do not converge to e_M. The input parameter γ in the corresponding "b" subcases was $\gamma = 0.001$, whereas in the corresponding "a" subcases $\gamma = 0.01$. Therefore, in the "a" subcases, the algorithm accounted for disturbances with larger time derivatives. Hence, the re-entry errors in the "a" subcases were more conservative than the "b" subcases.

TABLE I
COMPARISON BETWEEN SIMULATION CASES

Cases	Avg. Δt_i^u [s]	Percent increase† [%]	Num. re-entries
Case 1	0.99	-	249
Case 2a	1.92	193	127
Case 2b	2.27	228	106
Case 3a	2.04	206	120
Case 3b	2.55	256	95

†The percent increase is relative to the nominal dwell time in (14).

To highlight the main outcomes of the conducted simulation study, Table I displays the average dwell-time condition, percent increase in the dwell-time condition of Algorithm 1 [relative to the nominal dwell-time condition in (14)], and the number of re-entries to the feedback region in each simulation case. Across all simulation cases, the developed algorithm increased the maximum dwell-time condition by more than twofold. Moreover, the algorithm adapted to variations in the disturbance while ensuring the dead-reckoning errors did not exceed the maximum error threshold.

V. CONCLUSION

This article examines a class of Relay-Explorer problems where a single-agent system was tasked with following a desired path that was in a feedback-denied region. A dwell-time update mechanism was developed that leveraged intermittent output measurement data to compute a relaxed dwell-time condition. Lyapunov-based switched system methods were used to guarantee that the state tracking error was bounded to a prescribed maximum error threshold. Moreover, the developed dwell-time update mechanism was analyzed to show that the generated dwell times were less conservative than the nominal dwell time from prior works. To demonstrate the efficacy of Algorithm 1, comparative numerical simulations were conducted. Compared to the nominal dwell time in (14), the dwell times generated from Algorithm 1 increased more than twofold. Based on the simulation results in Section IV, the integration of intermittent data measurements in Algorithm 1 showed an increase in the dwell time and extended the agent's duration in the dead-reckoning mode. For clarity of the central idea, the problem setting in this technical note considered a single agent system. Future research efforts may investigate applications of the developed dwell-time update mechanism for multiagent settings. Natural challenges arise in the design and analysis of the developed algorithm when considering coordination of updates among a network of agents. Such challenges can include various graph topologies, asynchronous exchanges of information, and fidelity of shared information.

ACKNOWLEDGMENT

Any opinions, findings, and conclusions or recommendations expressed in this material are those of the author(s) and do not necessarily reflect the views of the sponsoring agency.

REFERENCES

[1] B. Jia and S. Liu, "Homography-based visual predictive control of tracked movile robot with field-of-view constraints," *Int. J. Robot. Automat.*, vol. 30, no. 5, 2015.

[2] A. J. Davison, I. D. Reid, N. D. Molton, and O. Stasse, "MonoSLAM: Real-time single camera SLAM," *IEEE Trans. Pattern Anal. Mach. Intell.*, vol. 29, pp. 1052–1067, Jun. 2007.

[3] B. Williams, M. Cummins, J. Neira, P. Newman, I. Reid, and J. Tardós, "A comparison of loop closing techniques in monocular SLAM," *Robot. Auton. Syst.*, vol. 57, no. 12, pp. 1188–1197, 2009.
[4] C. Cadena et al., "Past, present, and future of simultaneous localization and mapping: Towards the robust-perception age," *IEEE Trans. Robot.*, vol. 32, no. 6, pp. 1309–1332, Dec. 2016.
[5] S. Kluge, K. Reif, and M. Brokate, "Stochastic stability of the extended Kalman filter with intermittent observations," *IEEE Trans. Autom. Control*, vol. 55, no. 2, pp. 514–518, Feb. 2010.
[6] L. Li and Y. Xia, "Stochastic stability of the unscented Kalman filter with intermittent observations," *Automatica*, vol. 48, no. 5, pp. 978–981, 2012.
[7] B. Sinopoli, L. Schenato, M. Franceschetti, K. Poolla, M. Jordan, and S. Sastry, "Kalman filtering with intermittent observations," *IEEE Trans. Autom. Control*, vol. 49, no. 9, pp. 1453–1464, Sep. 2004.
[8] W. Heemels, K. Johansson, and P. Tabuada, "An introduction to event-triggered and self-triggered control," in *Proc. IEEE Conf. Decis. Control*, 2012, pp. 3270–3285.
[9] X. Yi, K. Liu, D. V. Dimarogonas, and K. H. Johansson, "Dynamic event-triggered and self-triggered control for multi-agent systems," *IEEE Trans. Autom. Control*, vol. 64, no. 8, pp. 3300–3307, Aug. 2019.
[10] H.-Y. Chen, Z. I. Bell, P. Deptula, and W. E. Dixon, "A switched systems framework for path following with intermittent state feedback," *IEEE Control Syst. Lett.*, vol. 2, pp. 749–754, Oct. 2018.
[11] F. Zegers, H.-Y. Chen, P. Deptula, and W. E. Dixon, "A switched systems approach to consensus of a distributed multi-agent system with intermittent communication," in *Proc. Am Control Conf.*, 2019, pp. 2372–2377.
[12] R. Sun, Z. Bell, F. Zegers, and W. E. Dixon, "A switched systems approach to unknown environment exploration with intermittent state feedback for nonholonomic systems," in *Proc. Amer. Control Conf.*, 2020, pp. 5275–5280.
[13] R. Sun, C. Harris, Z. Bell, and W. E. Dixon, "Relay-explorer approach for multi-agent exploration of an unknown environment with intermittent communication," in *Proc. IEEE Conf. Decis. Control*, 2020, pp. 5218–5223.
[14] Z. Xu, F. M. Zegers, B. Wu, W. E. Dixon, and U. Topcu, "Controller synthesis for multi-agent systems with intermittent communication: A metric temporal logic approach," in *Proc. Allerton Conf. Commun. Control Comput.*, . 2019, pp. 1015–1022.
[15] D. Le, H.-Y. Chen, A. R. Teel, and W. E. Dixon, "Path following with stable and unstable modes subject to time-varying dwell-time conditions," in *Proc. IFAC World Congr.*, 2020, pp. 6440–6445.
[16] H.-Y. Chen, Z. Bell, P. Deptula, and W. E. Dixon, "A switched systems approach to path following with intermittent state feedback," *IEEE Trans. Robot.*, vol. 35, no. 3, pp. 725–733, Jun. 2019.
[17] R. Goebel, R. G. Sanfelice, and A. R. Teel, *Hybrid Dynamical Systems*. Princeton, NJ, USA: Princeton Univ. Press, 2012.
[18] R. Goebel, R. G. Sanfelice, and A. R. Teel, "Hybrid dynamical systems," *IEEE Control Syst. Mag.*, vol. 29, no. 2, pp. 28–93, Apr. 2009.
[19] D. Liberzon, *Switching in Systems and Control*. Cambridge, MA, USA: Birkhauser, 2003.
[20] J. P. Hespanha and A. S. Morse, "Stability of switched systems with average dwell-time," in *Proc. IEEE Conf. Decis. Control*, 1999, pp. 2655–2660.
[21] C. Cai, A. Teel, and R. Goebel, "Smooth Lyapunov functions for hybrid systems part II: (Pre)asymptotically stable compact sets," *IEEE Trans. Autom. Control*, vol. 53, no. 3, pp. 734–748, Apr. 2008.
[22] J. P. Hespanha, D. Liberzon, and A. R. Teel, "Lyapunov conditions for input-to-state stability of implusive systems," *Automatica*, vol. 44, pp. 2735–2744, Nov. 2008.
[23] M. A. Müller and D. Liberzon, "Input/output-to-state stability and state-norm estimators for switched nonlinear systems," *Automatica*, vol. 48, no. 9, pp. 2029–2039, 2012.
[24] G. Yang and D. Liberzon, "Input-to-state stability for switched systems with unstable subsystems: A hybrid Lyapunov construction," in *Proc. IEEE Conf. Decis. Control*, 2014, pp. 6240–6245.
[25] G. Yang and D. Liberzon, "A Lyapunov-based small-gain theorem for interconnected switched systems," *Syst. Control Lett.*, vol. 78, pp. 47–54, 2015.
[26] J. I. Poveda and A. R. Teel, "A framework for a class of hybrid extremum seeking controllers with dynamic inclusions," *Automatica*, vol. 76, pp. 113–126, Feb. 2017.
[27] X.-F. Wang, A. R. Teel, K.-Z. Liu, and X.-M. Sun, "Stability analysis of distributed convex optimization under persistent attacks: A hybrid systems approach," *Automatica*, vol. 111, 2020, Art. no. 108607.
[28] X.-F. Wang, X.-M. Sun, A. R. Teel, and K.-Z. Liu, "Distributed robust Nash equilibrium seeking for aggregative games under persistent attacks: A hybrid systems approach," *Automatica*, vol. 122, 2020, Art. no. 109255.
[29] S. Edwards, D. Le, D. Guralnik, and W. E. Dixon, "A topologically inspired path-following method with intermittent state feedback," *IEEE Robot. Automat. Lett.*, vol. 6, no. 3, pp. 4449–4456, Jul. 2021.
[30] H. K. Khalil, *Nonlinear Systems*, 3rd ed. Englewood Cliffs, NJ, USA: Prentice Hall, 2002.